DsbA-L interacts with VDAC1 in mitochondrion-mediated tubular cell apoptosis and contributes to the progression of acute kidney disease

Xiaozhou Li,[a,b,1] Jian Pan,[a,b,1] Huiling Li,[c] Guangdi Li,[g] Bohao Liu,[a,b] Xianming Tang,[a,b] Xiangfeng Liu,[f] Zhibiao He,[a,b] Zhenyu Peng,[a,b] Hongliang Zhang,[a,b] Luxiang Wang,[a,b] Yijian Li,[d] Xudong Xiang,[a,b] Xiangping Chai,[a,b] Yunchang Yuan,[e] Peilin Zheng,[h] and Dongshan Zhang [a,b]*

[a]Department of Emergency Medicine, People's Republic of China
[b]Emergency Medicine and Difficult Diseases Institute, Second Xiangya Hospital, Central South University, Changsha, Hunan 410011, People's Republic of China
[c]Department of Ophthalmology, People's Republic of China
[d]Departmentof Urinary Surgery, People's Republic of China
[e]Department of Chestsurgery, People's Republic of China
[f]Department of General Surgery, Second Xiangya Hospital, People's Republic of China
[g]Department of Public Health, Central South University, Changsha, Hunan, People's Republic of China
[h]Department of Endocrinology, Shenzhen People's Hospital, The Second Clinical Medical College of Jinan University, The First Affiliated Hospital of Southern University of Science and Technology, Shenzhen, People's Republic of China

eBioMedicine 2022;76: 103859
Published online xxx
https://doi.org/10.1016/j.ebiom.2022.103859

Summary

Background we demonstrated that disulfide-bond A oxidoreductase-like protein (DsbA-L) was involved in the progression of renal fibrosis. However, the precise function of DsbA-L in acute kidney injury (AKI), and the mechanisms involved, have yet to be elucidated.

Methods We illustrate the DsbA-L interacted with VDAC1 by co-IP (co-immunoprecipitation) *in vitro* and *vivo*, and found the interaction parts of them by mutation experiment. The above findings were verified by co-localization of them. In addition, we constructed the two model of PT-DsbA-L and VDAC1 KO mice to verify the function of DsbA-L and VDAC1 in models of VAN, CLP and I/R-induced AKI.

Findings The PT-DsbA-L-KO mice showed amelioration of I/R, VAN-, and CLP-induced AKI progression via the downregulation of VDAC1. Finally, we confirmed these changes in signal molecules by examining in HK-2 cells and kidney biopsies taken from patients with ischemic or acute interstitial nephritis (AIN)-induced AKI. Mechanistically, DsbA-L interacted with amino acids 9−13 and 22−27 of VDAC1 in the mitochondria of BUMPT cells to induce renal cell apoptosis and mitochondrial injury.

Interpretation This work suggested that DsbA-L, located in the proximal tubular cells, drives the progression of AKI, by directly upregulating the levels of VDAC1.Running Title: The role of DsbA-L in AKI

Funding National Natural Science Foundation of China, a grant from Key Project of Hunan provincial science and technology innovation, Department of Science and Technology of Hunan Province project of International Cooperation and Exchanges, Changsha Science and Technology Bureau project, Natural Science Foundation of Hunan Province, Fundamental Research Funds for the Central Universities of Central South University, Hunan Provincial Innovation Foundation For Postgraduate China Hunan Provincial Science and Technology Department.

Keywords: DsbA-L; VDAC1; Bax; Cyt-c; AKI

*Corresponding author at: Emergency Medicine and Difficult Diseases Institute, Second Xiangya Hospital, Central South University, Changsha, Hunan 410011, People's Republic of China.
E-mail address: dongshanzhang@csu.edu.cn (D. Zhang).

[1] Xiaozhou Li and Jian Pan contributed equally to this study

Research in context

Evidence before this study

Disulfide-bond A oxidoreductase-like protein (DsbA-L) was firstly identified as a mitochondria protein in rat liver cells.[13] Recent studies reported that DsbA-L protested against diet or diabetic nephropathy (DN)-induced obesity, inflammation, insulin resistance, or kidney injury.[14–18] Furthermore, our recent study verified that DsbA-L mediated unilateral ureteral obstruction (UUO)-induced renal fibrosis. However, the role and mechanism of tubular DsbA-L in AKI is still completely unknown.

Added value of this study

Our data show that DsbA-L interacted with VDAC1 to induce mitochondrial damage to promote renal cell apoptosis, and finally drive the progression of AKI. In addition, DsbA-L interaction with VDAC1 could be considered as a potential therapeutic target to attenuate the pathological mitochondrial effects caused by AKI.

Implications of all the available evidence

In the present study, we demonstrated that a proximal tubule-specific DsbA-L knockout mouse (PT-DsbA-L-KO) showed amelioration of I/R, CLP, and VAN-induced renal function decline, renal cell apoptosis, and mitochondrial damage. Mechanistically, DsbA-L interacted with amino acids 9-13 and 22-27 of VDAC1. Furthermore, a proximal tubule-specific VDAC1 knockout mouse (PT-VDAC1-KO) showed attenuation of I/R, CLP, and VAN-induced renal function decline, renal cell apoptosis, and mitochondrial damage. In additional, the PT-DsbA-L-KO mice showed amelioration o f I/R, VAN-, and CLP-induced AKI progression via the downregulation of VDAC.

Introduction

Acute kidney injury (AKI), a devastating clinical complication with high rates of morbidity and mortality, affects millions of patients across the entire world(1). AKI is usually induced by sepsis, nephrotoxic agents, and ischemia-reperfusion injury (IRI)(2). As yet, the molecular mechanisms underlying AKI have yet to be fully elucidated. Consequently, there are no effective treatment strategies available for AKI.

Tubular cell injury has been recognized for decades as an important driver of AKI.[3] As research has progressed, an increasing number of researchers have identified that mitochondrial damage plays a key role in tubular cell injury and that this initial damage is caused by the accumulation of ROS, the production of cytokines, and cellular death (including both necrosis and apoptosis); collectively, these processes all contribute to AKI.[4–6] Although a growing body of research has focused on the mechanisms underlying mitochondrial damage in AKI,[7–12] the precise mechanism responsible for mitochondrial injury has yet to be identified.

Disulfide-bond A oxidoreductase-like protein (DsbA-L) was firstly identified as a mitochondria protein in rat liver cells.[13] Previous studies have demonstrated that DsbA-L prevented diet or diabetic nephropathy (DN)-induced obesity, inflammation, insulin resistance, or kidney injury.[14–18] Interestingly, our recent study found that DsbA-L mediated unilateral ureteral obstruction (UUO)-induced renal fibrosis. However, the role and mechanism of tubular DsbA-L in AKI is still completely unknown.

In the present study, the proximal tubular deletion of DsbA-L (PT-DsbA-L-KO) in a mouse model resulted in the notable attenuation of I/R, along with vancomycin (VAN)- and cecal ligation and puncture (CLP)-induced AKI. Consistently, DsbA-L also mediated I/R, VAN-, and LPS-induced apoptosis in mouse renal proximal tubular epithelial (BUMPT) cells. Interestingly, we found that DsbA-L interacted with the 9−13 and 22−27 regions of the voltage-dependent anion channel 1 (VDAC1), a key member of the VDAC family of proteins[19–21]; these effects were observed in both *in vivo* and *in vitro* mitochondrial samples and in human AKI samples. Furthermore, we demonstrated that PT-VDAC1-KO also ameliorated renal cell apoptosis in both *in vitro* and *in vivo* models of AKI. Collectively, we demonstrated that DsbA-L interacted with VDAC1 in mitochondrion-mediated tubular cell apoptosis and therefore caused the progression of AKI.

Materials and methods

Ethics statement

The study was approved by the Review Board of the Second Xiangya Hospital, People's Republic of China (NO. 2018065) and this study recruited 18 patients. All participants prior to inclusion in the study were recruited with written informed consent. All animal experiments complied with the guiding principles approved by the Animal Care Ethics Committee of Second Xiangya Hospital, People's Republic of Chinae (NO. 2020310).

Antibodies and reagents

Anti-COXIV (ab33985, RRID: AB_879754), VDAC1 (ab14734, RRID: AB_443084) and PGC-1α (ab191838, RRID: AB_2721267) antibodies were obtained from Abcam (Cambridge Science Park, Cambridge, UK). Anti-Caspase3 (9662, RRID: AB_331439) and cleaved-capase3 (9664, RRID: AB_2070042) antibodies were purchased from Cell Signaling Technology (Danvers, MA, USA). Anti-Bax (50599-2-Ig, RRID: AB_2061561) , Cyt-c (10993-1-AP, RRID:AB_2090467) , NRF1 (12482-1-AP, RRID: AB_2282876), GAPDH (60004-1-Ig, RRID: AB_2107436), and β-tubulin (10094-1-AP, RRID: AB_2210695) antibodies were obtained from Proteintech (Rosemont, IL, USA). The anti-DsbA-L

antibody was provided by Dr. Feng Liu(14). All secondary antibodies (MitoTracker Green FM and MitoTracker Red CMXRos) were obtained from Thermo Fisher Scientific (Waltham, MA, USA). The calcium ionophore was purchased from Sigma-Aldrich (Shanghai, China). Antimycin A (>95% pure, ab141904) and a Mitochondria/Cytosol Fractionation Kit (ab65320) were purchased from Abcam (Cambridge Science Park, Cambridge, UK). The target sequence for mouse DsbA-L has been described previously.[22]

The creation of AKI models by ischemic reperfusion, CLP, and VAN

C57BL/6J male mice (RRID: MGI:5657312) aged 8-10 weeks were purchased from Hunan SJA Laboratory Animal Co., Ltd. Mice exhibiting proximal tubule-specific DsbA-L or VDAC1 deletion were produced by crossing DsbA-L (flox/flox) mice (provided by Dr. Feng Liu) or VDAC1 (flox/flox) mice (obtained from Shanghai model organisms) with PEPCK-Cre mice (provided by Dr. Volker Haase (University of Pennsylvania, Philadelphia, PA) as described previously.[22,23] Male mice (8-10 weeks of age) were subjected to ischemia, CLP, and VAN nephrotoxic AKI, as described previously.[23–27] For ischemic AKI, the bilateral renal artery was continuously clipped for 28 min followed by reperfusion for 24 h or 48 h. The body temperature of the mice was maintained at approximately 37°C. For CLP-induced AKI, the cecum was tightly ligated at a position 1.5 cm from the tip. This was followed by puncture for 18 h. For VAN injury, mice were intraperitoneally injected with a single dose of VAN at a dose of 600 mg/kg for 7 consecutive days, as described previously.[28,29] In additional, the C57BL/6 mice were injected with DsbA-L or VDAC1 plasmids, or VDAC1 siRNA (at a dose of 15 mg/kg) via the tail vein twice a week[22]; saline was used as a control injection. For each study, we analyzed the samples together to avoid bias, based on previous study and used the PASS software to determine the sample size(n=6). We excluded the sample that died or failed the model establishment before endpoint. The experimental mice were grouped by random-numbers table. Investigators were not blinded during carrying out the experiment, but blinded during the allocation, sample collection, and data analysis. All animal experiments complied with the guiding principles approved by the Animal Care Ethics Committee of Second Xiangya Hospital, People's Republic of China. Mice were housed in a 12-h light/dark environment with free access to a standard rodent diet and water.

Cell culture and an ischemia reperfusion model

BUMPT cells obtained from Dr. Wilfred Lieberthal (Boston University School of Medicine) or HK-2 cells obtained from Shanghai Zhongqiaoxinzhou Biotech were cultured with DMEM (Gibco, 11965092) added 10% FBS (Gibco,10100147) and 1% Penicillin-Streptomycin(Gibco, 15140163) at 37°C in 5% CO2. For the ischemic cell model, BUMPTs cells were treated with 10μM antimycin A (an inhibitor of mitochondrial complex III, Abcam, ab141904) and 1.5μM calcium ionophore (Sigma, A23187) in Hanks' Balanced Salt Solution (Hyclone, SH30030.02) for 2 h.[30] We then replaced HBSS with DMEM medium for 0, 2, 4 h for the reperfusion stage. Cell apoptosis was detected by morphology and immunoblotting for apoptotic indicators, including cleaved-caspase3, Bax, and Cyt-c. Several plasmids were created and transfected into cells by lipofection: DsbA-L, HA-VDAC1-1-25, HA-VDAC1-26-366, HA-VDAC1-full length, HA- VDAC1-Δ9-13,22-27, HA-VDAC1-Δ39-45,55-57, and HA- VDAC1-Δ9-13,22-27 Δ39-45,55-57, and siRNA for DsbA-L and VDAC1. Six to eight hours after transfection, the culture medium was replaced with DMEM. The sequences of DsbA-L siRNA and VDAC1 siRNA for mouse were 5′- GCAUGGAGCAACCAGAGAUTT -3′ and 5′- CCAGAGCAACTTCGCAGTT -3′, respectively; the sequences for the scrambled NC siRNA were 5′-UUCUCCGAACGUGUCACGUTT-3′. The sequences of DsbA-L siRNA and VDAC1 siRNA for human were 5′- UCAUUUGCCAUGUAUAGUCCU-3′ and 5′-UAUUAAGCCAAAUCCAUAGCC -3′, respectively; the sequences for the scrambled NC siRNA were 5′-AACCACUCAACUUUUUCC CAA -3′. The model of IR was then induced when the cell density reached 90%.

Flow cytometry

The flow cytometry was operated according the instruction of the FITC Annexin V Apoptosis Detection Kit (BD, 556547). BUMPT or HK-2 Cells with different treatment were collected using trypsin without EDTA, and washed three times with PBS followed by the FITC for 15min and PI for 5min at room temperature, and finally examined by the flow cytometry.

AKI patients and sample collection

The protocol was approved by the Review Board of the Second Xiangya Hospital, People's Republic of China. This study recruited 18 patients, including 12 males and 6 females. The recruitment principle was based on kidney biopsy. Patient information is supplemented in Table 1. The kidney biopsy specimens were obtained from patients living with minimal change diseases (MCD) (n=6) and ischemic or acute interstitial nephritis (AIN)-induced AKI (n=6). We declare that all study complies with all relevant ethical regulations for research with human participants and was carried out in compliance with the Declaration of Helsinki principles, and that the study is compliant with the guidance of the Ministry of Science and Technology for the

Characteristics MCD (n=6)	IR (n=6) AIN (n=6)
Age(years)(mean)[SD] 52.51 (3.95)	50.32(3.58) 55.92(4.28)
Gender	
male 5	3 4
female 1	3 2
BMI(mean)[SD] 22.01(0.92)	20.35(0.62) 23.15(0.57)
Diagnosis minimal change diseases	Ischemia reperfusion acute interstitial nephritis
Biopsy side	
Left 2	5 3
Right 4	1 3
Blood urea nitrogen(mM) 5.28 (0.63) (mean)[SD]	13.56(0.42) 14.29(0.31)
Serum creatinine(uM) 72.71 (3.46) (mean)[SD]	192. 09(5.31) 183. 09 (4.09)

***Table 1*: The basic clinical information of MCD, IR and AIN patients.**

Review and Approval of Human Genetic Resources. Inclusion and exclusion criteria of MCD was described as our previous study.[23] For IR: Inclusion criteria:[1] Biopsy for ischemia-reperfusion patients,[2] Age less than 75 years old; Exclusion criteria[1]: exclude patients with tumors found in postoperative medical examinations,[2] exclude patients with a history of diabetes, gout, hypertension, urinary tuberculosis or infection respectively. For AIN: Inclusion criteria[1]: Clinically diagnosed as acute interstitial nephritis[2] Biopsy confirmed AIN patients,[3] Age less than 75 years old; Exclusion criteria[1]: Exclude patients with abnormal blood creatinine before admission,[2] exclude patients with a history of diabetes, gout, hypertension, urinary tuberculosis or infection. These specimens were then used for staining of HE, TUNEL, and immunohistochemistry as well as immunoprecipitation (IP) and immunoblotting.

Immunoprecipitation

The cytoplasm and mitochondria from BUMPT cells and kidney tissue from mice and AKI patients were separated using the Mitochondria/Cytosol Fractionation Kit (Abcam, ab65320); the kit was used in accordance with the manufacturer's instructions. The antibodies (DsbA-L, VDAC1, HA or IgG) were bound onto the magnetic beads. Next, we added the mitochondria/cytoplasm lysate and incubated for three hours. Next, the mixture was eluted and investigated for the expression of associated markers by immunoblotting.

Relative quantitative PCR (qPCR)

RNA was extracted from BUMPT cells or kidney tissue by the Trizol reagent (Invitrogen, Carlsbad, CA, USA). RNA was then reverse-transcripted into first-strand cDNA using the Prime Script RT Reagent kit and gDNA Eraser (TaKaRa, RR037A), as previously described.[31–34] Next, we used the cDNA as a template with TB green (TaKaRa, RR820A) and a Light cycler 96 (Roche) with the following primer pairs: DsbA-L: 5-AAATATGGGGCCTT TGGGCT-3´ (forward) and 5-TAGCAACTCCAAGCGGTCA G-3´ (reverse); and GAPDH: 5-GGTCTCCTCTGACTTCACA-3´ (forward) and 5-GTGAGGGTC TCTCTCTTCCT-3(reverse);PGC-1α: 5'-ATGTGTCGCCTTCTTGCTCTTCC-3 (forward) and 5'-CTCCCGCTTCTCGTGCTCTTTG-3(reverse); NrF1:5'-TCTGCTGTGGCTGATGGAGA GG-3(forward) and NrF1:5'-GATGCTTGCGTCGTCTGGATGG-3 (reverse);

BUN and creatinine detection

The detection of BUN and creatinine was performed according to the protocol of BUN (Urea Nitrogen Content Assay Kit Beijing Boxbio Science & Technology Co, Ltd.) and Creatinine Assay kit(Nanjing Jiancheng Bioengineering Institute, Nanjing, China).

HE staining, TUNEL staining, immunochemistry, immunofluorescence, and immunoblotting

Renal tissue was embedded in paraffin and then cut into sections for various types of staining, as described previously.[26,35] Histology was assessed by hematoxylin and eosin staining. The criteria used to score renal tubular injury were described previously.[23] TUNEL staining was used to evaluate apoptosis in the renal cells. The proportion (%) of TUNEL-positive cells in 10-20 microscopic fields per tissue section was used as a quantitative indicator of apoptosis.[26] For immunochemistry staining, tissue sections were incubated overnight at 4° C with specific primary antibody (DsbA-L 1:200 or VDAC1 1:100). The following morning, the sections were incubated with secondary antibody for 30min at 37°C and then reacted with DAB for 5-10 min. For immunofluorescence staining, the sections were incubated with specific primary antibody (DsbA-L 1:200, VDAC1 1:100) overnight at 4°C followed by a secondary fluorescent antibody for 1 h at 37°C in the dark. DAPI was then added for 3-5 min and the sections observed by fluorescent microscopy. Mitochondrial staining was performed in accordance with a standard protocol. Protein lysates from BUMPT cells or kidneys were harvested and then centrifuged to collect the supernatant containing the proteins. The supernatant was subjected to SDS-PAGE and then transferred to a PVDF membrane. The membranes were then incubated with primary antibody overnight at 4°C followed by a secondary antibody for 1 h at room temperature. The concentration of anti-COXIV, VDAC1, PGC-1α, Bax, Cyt-c, NRF1, GAPDH, and β-tubulin is 1:1000. The concentration of anti−Caspase3 and cleaved-capase3 is 1:2000.

Statistics

All data were presented as means ± SD. Two-tailed Student t-tests was used for two group comparisons. One-way ANOVA followed by Tukey's post hoc analysis was used for multiple comparisons. The Kruskal–Walls test was used the data with non-normal distribution. The Graph Pad software 8.0 was used to analysis the data and $P<0.05$ was considered statistically significant.

Role of funding source

The funders were not involved in study design, data collection, analysis, interpretation or writing of the manuscript.

Results

Ischemic injury induced the expression of DsbA-L in BUMPT cells and the kidneys of mice and patients

To investigate whether ischemic injury induced the expression of DsbA-L, we depleted BUMPT cells of ATP for 2 h, and then allowed them to recover for a total period of 4 h. RT-qPCR and immunoblotting results indicated that the expression of DsbA-L was induced at I/R 2-0, reached a peak at I/R 2-2, and then gradually reduced to levels seen at I/R 2-0 (Figure 1a, e and i). Immunofluorescence staining of DsbA-L further confirmed these findings and indicated that DsbA-L is predominantly expressed in the cytoplasm of BUMPT cells (Figure 1 m and n). We further detected the expression of DsbA-L in C57BL/6 mice treated with ischemia (28 min) and reperfusion injury (24 h and 48 h). RT-qPCR and immunoblotting results indicated that the expression of DsbA-L was induced in both the cortex and outer medulla of the mice kidney after 24 h of reperfusion and reached a peak 48 h after reperfusion (Figure 1 b, c, f, g, j and k). These findings were further confirmed by the immunohistochemical staining of DsbA-L (Figure 1 o and p). Finally, we investigated whether the expression levels of DsbA-L were induced in patients with AKI caused by ischemia. These results indicated that the levels of DsbA-L mRNA and protein were notably increased in patients with AKI caused by ischemia when compared to MCD patients (Figure 1. d, h and l). These results were further validated by the immunofluorescence staining of DsbA-L (Figure 1. q and r).

IR-induced renal injury, tubular cell apoptosis, and mitochondrial damage was attenuated in PT-DsbA-L-KO mice

The littermates of PT-DsbA-L-WT and PT-DsbA-L-KO mice were treated with or without ischemia (28 min) and reperfusion injury (24 h and 48 h). Following this treatment, we acquired blood samples and samples of kidney tissues for further examination. Functionally, I/R-induced renal function deterioration was characterized by increasing levels of blood urea nitrogen (BUN) and creatinine in the PT-DsbA-L-WT mice; this effect was significantly attenuated in the PT-DsbA-L-KO mice (Figure 2a and b). Histology and TUNEL analyses also verified that I/R-induced notable tissue damage and apoptosis in the PT-DsbA-L-WT mice, although this was ameliorated in the PT-DsbA-L-KO mice (Figure 2c,d,f and g). Interestingly, electron microscopy (EM) analyses indicated that PT-DsbA-L-KO mice showed marked attenuation of the I/R-induced mitochondrial damage (Figure 2 e and h). Immunoblotting further verified that PT-DsbA-L-KO mice also expressed lower levels of cleaved caspase-3, lower accumulation rates of Bax in the mitochondria, and reduced levels of cytochrome c (Cyt-c) release into the cytosol (Figure 2 i–o). RT-qPCR analysis results demonstrated that PT-DsbA-L-KO reversed the reduction of NRF1 and PCG-1α caused by the I/R(Figure 2 p and q), which was further confirmed by the immunoblotting analysis (Figure 2 r–t). These data showed that DsbA-L played a pivotal role in I/R-induced AKI.

DsbA-L mediated I/R induced apoptosis in BUMPT cells

To further investigate whether DsbA-L mediates apoptosis in BUMPT cells induced by I/R, we transfected BUMPT cells with DsbA-L siRNA and then depleted these cells from ATP for 2 h; the cells were then allowed to recover for 2 h. FCM analyses found that DsbA-L siRNA significantly attenuated I/R-induced apoptosis in BUMPT cells (Figure 3a). Immunoblotting analyses further confirmed that DsbA-L siRNA notably suppressed the I/R-induced increase in cleaved caspase-3 expression, the increased accumulation of Bax in the mitochondria, and the increased release of Cyt-c into the cytosol (Figure 3 b–h). RT-qPCR analysis results showed that I/R-suppressed the expression of NRF1 and PCG-1α, which was reversed by the DsbA-L siRNA (Figure 3 i and j). The immunoblotting results were consistent with the findings of RT-qPCR (Figure 3 k–m). In contrast, the DsbA-L plasmid enhanced I/R-induced apoptosis in BUMPT cells, increased the expression of cleaved caspase-3, increased the accumulation of Bax, and increased the release of Cyt-c into the cytosol (Figure 3 o–u). RT-qPCR analysis results indicated that I/R-suppressed the expression of NRF1 and PCG-1α, which was enhanced by the DsbA-L plasmid (Figure 3 v and w). The immunoblotting results further confirmed the findings of RT-qPCR (Figure 3 x–z). These data further confirmed that DsbA-L-mediated the process of apoptosis as well as mitochondrial dysfunction during ischemic injury.

DsbA-L interacted with VDAC1 in BUMPT cells that had been subject to ATP depletion as well as in the kidneys of mice and patients with AKI

Previous results suggested that voltage-dependent anion channel-1 (VDAC1), an important protein of the outer

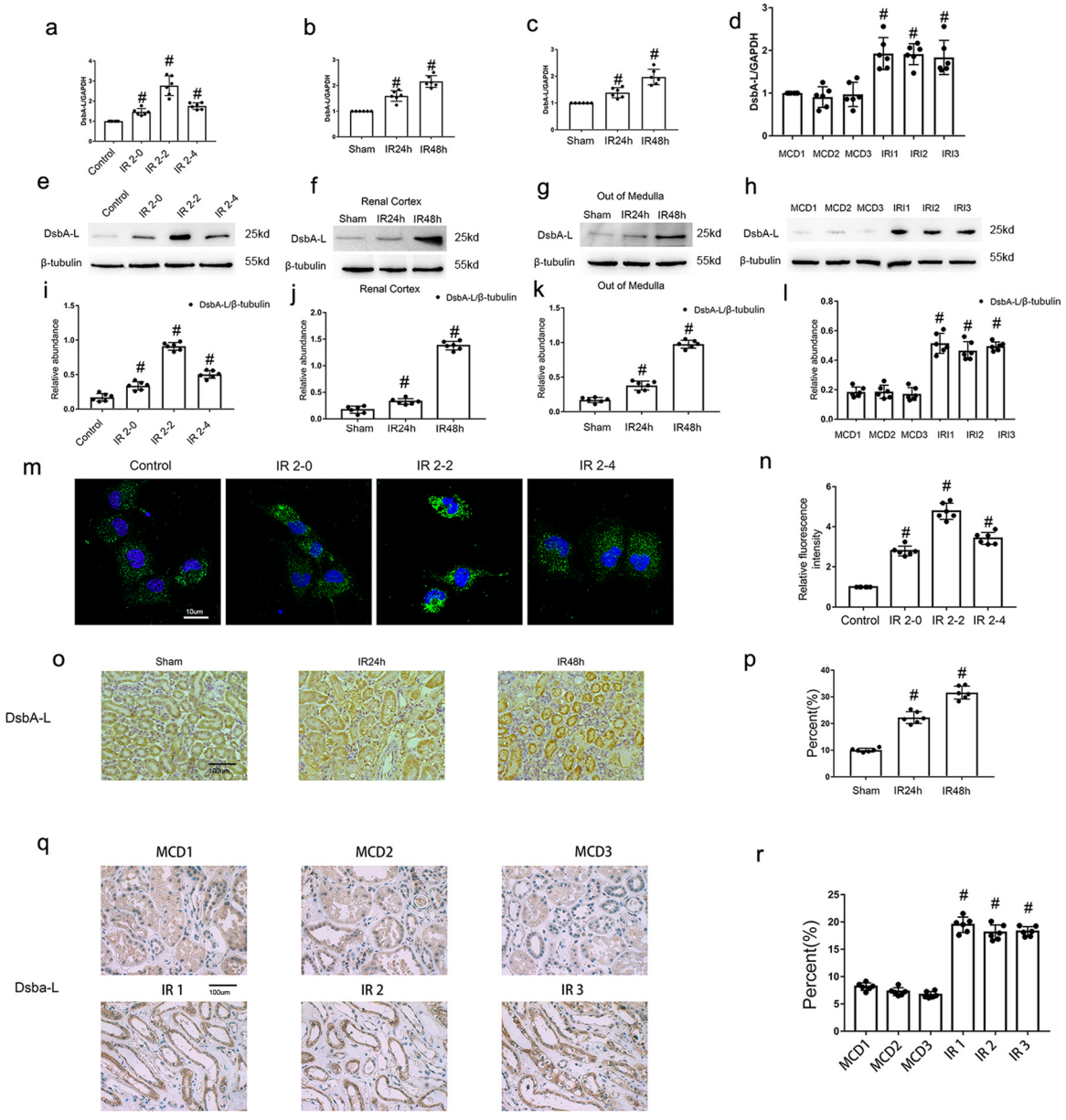

Figure 1. DsbA-L **was induced by I/R in BUMPT cells *and* kidneys of mice and patients**. I/R model in BUMPT cells was induced by 10 μM antimycin A and 1.5 μM calcium ionophore for 2 h and recover for 0, 2, and 4 h. I/R mice model was induced by bilateral renal ischemia for 28 min and reperfusion for 24 and 48 h. Renal biopsy samples were collected from I/R-induced AKI patients and Minimal Change Disease (MCD) patients. (a-d) RT-qPCR detection of DsbA-L expression in BUMPT cells, mice kidney cortical tissue and out of medulla and kidney patients with or without I/R condition. (e−h) Immunoblot analysis of DsbA-L and β-tubulin in BUMPT cells under I/R model in BUMPT cells, cortical tissue, out of medulla and kidney patients. (i−l) Densitometry analysis of DsbA-L and β-tubulin protein expression. (m, o and q) Immunofluorescence and immunohistochemical staining of DsbA-L in BUMPT cells and kidneys of mice and patients with or without I/R condition, respectively. (n, p, and r) Quantification analysis of DsbA-L staining. Original magnification x 400. Scar Bar:10μM in m100μM in o and q. Each experiment (e−h, m, o, and q) was repeated 6 times independently with similar results. Two-tailed Student t-tests was used for two group comparisons. (a−d,i−l, n, p and r). # $p<0.05$: versus saline group, sham group, or MCD group.

mitochondrial membrane, is involved in cell apoptosis[36] Our recent study reported that DsbA-L is also expressed in the mitochondria. Hence, we hypothesized that DsbA-L interacted with VDAC1 to regulate the progression of AKI. Immunoprecipitation (IP) results demonstrated that the anti-VDAC1 antibody pulled down both

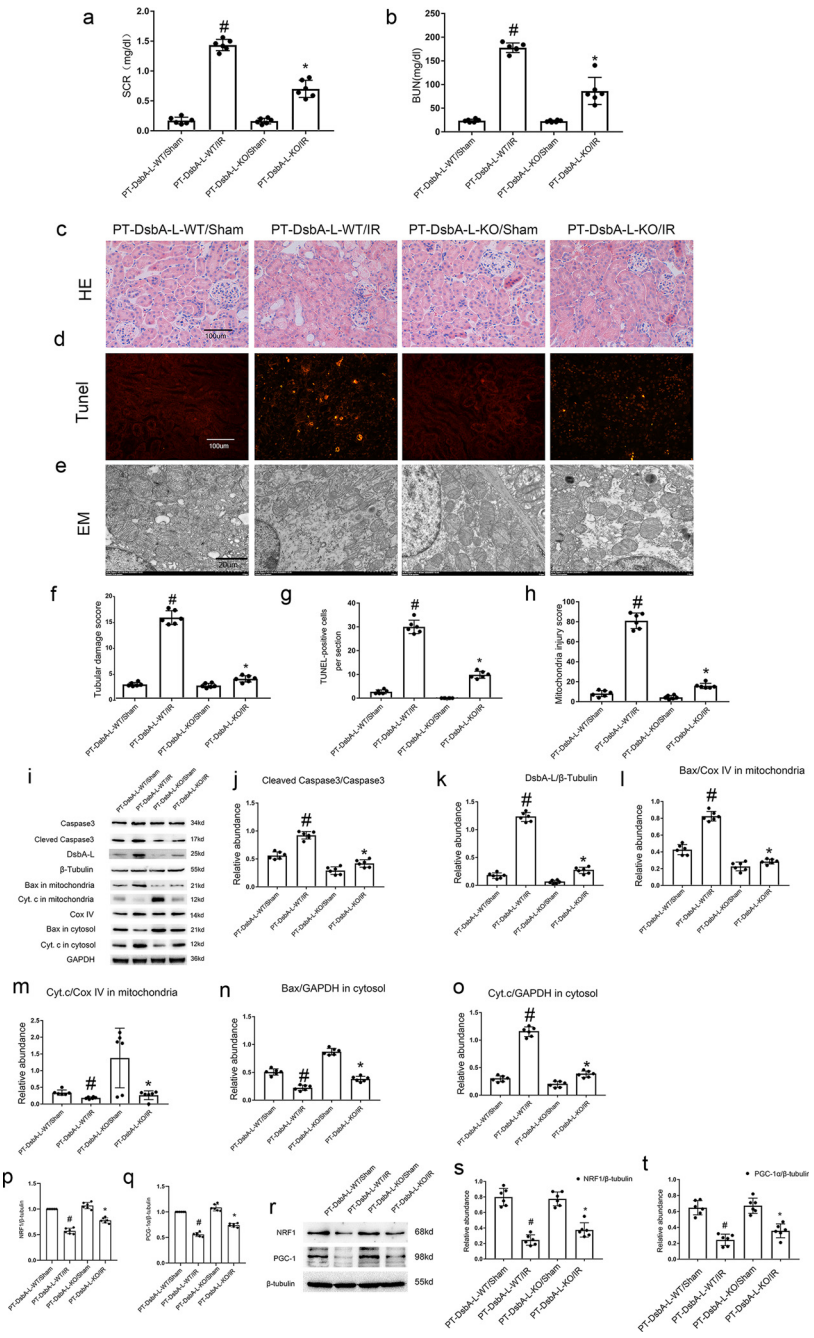

Figure 2. Attenuation of IR-induced renal injury, tubular cell apoptosis, and mitochondrion damage, and the expression of Bax, Cyt-c, and cleaved caspase3 in PT-DsbA-L-KO mice. The bilateral renal arteries of PT-DsbA-L-KO and PT-DsbA-L-WT littermate mice were clamped for 28min and then released for 48 h to establish an IR model. (a) BUN (b) Serum creatinine (c) Hematoxylin and eosin staining. (d) Representative sections of TUNEL-positive cells. (e) Electron microscope detection of mitochondrion morphology. (f) Tubular damage score. (g) The number of TUNEL-positive cells. (h) Mitochondria injury score. (i) The immunoblot analysis of the expression of cleaved caspase3 and DsbA-L, and the expression of BAX and Cyt-c in mitochondrial and cytosolic fractions. β-tubulin and GAPDH was used as whole lysate or cytosolic loading control, respectively. COX IV was used as mitochondria loading control. (j−o) Analysis of the gray scale image between them. (p and q) RT-qPCR detection of the expression of NRF1 and PCG-1α. (r) The immunoblot analysis of the expression of NRF1 and PCG-1α. (s and t) Analysis of the gray scale image between them. Original magnification x 400 or x6000. Scar Bar:100μM in c&d 20μM in e. Each experiment(c−e, i and r) was repeated 6 times independently with similar results. One-way ANOVA was used for the Multiple group comparisons. (a, b,f−h, j−o, p−q & s−t). # *p<0.05*: versus saline group, sham group, or MCD group. # $P<0.05$ versus sham group. * $P<0.05$ versus PT-DsbA-L-WT with IR group.

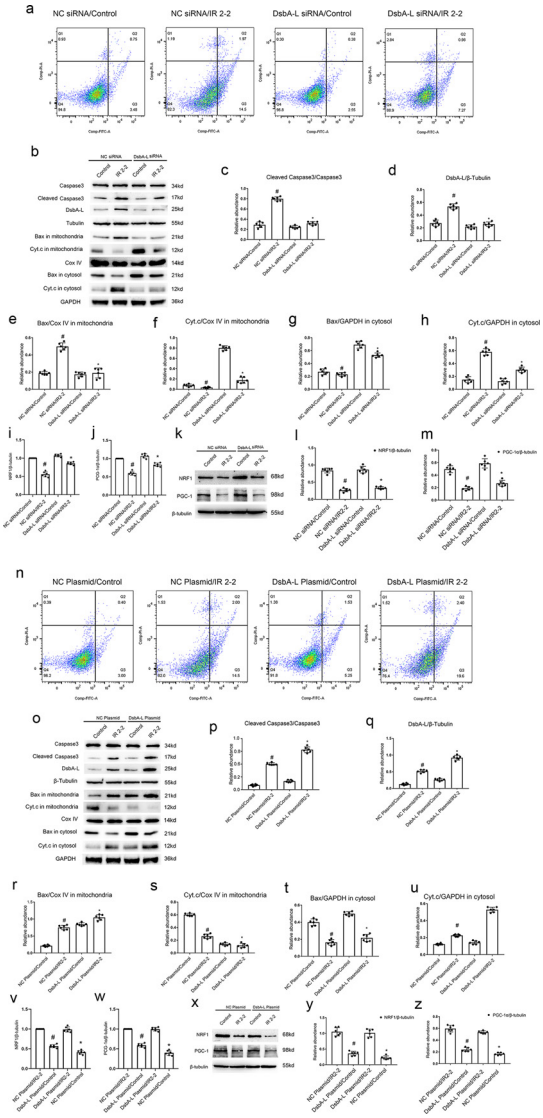

Figure 3. DsbA-L-mediated the IR-induced expression of cleaved caspase3, BAX, and Cyt-c in BUMPT cells. The plasmid and siRNA of DsbA-L were transfected into BUMPT cells and then exposed to ATP depletion for 2 h and recovery for 2 h. (a&n) Flow cytometry analysis of BUMPT cells apoptosis. (b&o) The immunoblots analysis the expression of cleaved caspase3 and DsbA-L, and the expression of BAX and Cyt-c in mitochondrial and cytosolic fractions. β-tubulin and GAPDH was used as whole lysate or cytosolic loading control, respectively. COX IV was used as mitochondria loading control. (c−h and q−u) Analysis of the gray scale image between them. (i,j and v, w) RT-qPCR detection the expression of NRF1 and PCG-1α. (k and x) The immunoblot analysis of the expression of NRF1 and PCG-1α. (l, m and y,z) Analysis of the gray scale image between them. Each experiment(a, b, k, n, o and x) was repeated 6 times independently with similar results. One-way ANOVA was used for the Multiple group comparisons. (c−j,c−m, p−w & y, z). # *p<0.05*: versus saline group, sham group, or MCD group. # *P<0.05* versus scramble with saline group. * *P<0.05* versus scramble with IR group.

VDAC1 and DsbA-L proteins, while anti-DsbA-L precipitated both DsbA-L and VDAC1 in whole lysates of control and I/R groups of BUMPT cells, and mice kidneys and patients kidneys (Figure 4a). Furthermore, the mitochondrial lysates of BUMPT cells, and mice kidneys and patients kidneys were also used for the co-IP of DsbA-L and VDAC1; findings were consistent with those for the whole lysate (Figure 4b). The structure of DsbA-L contains a nucleotide binding domain/ATPase domain (amino acids 1-51), amino-terminal domain (NTD), a helical region for dimerization (amino acids 56-178), and a carboxyl-terminal domain (CTD; amino acids 185-216) (Figure 4c). Based on the structure of VDAC1, software prediction indicated that the N-terminal domain (amino acids 1 to 25) of VDAC1 may interact with DsbA-L (Figure 4d). To clarify which domains of VDAC1are able to interact with DsbA-L, we constructed three plasmids for HA-VDAC1 featuring amino acids 1-75, amino acids 76-1098, and the full gene (Fig 4e). The anti-HA antibody precipitated DsbA-L in groups featuring VDAC1 with amino acids 1-75 and the full gene, but not with VDAC1 and the plasmid featuring amino acids 76-1098. This indicated that DsbA-L interacted with the region of VDAC1 that features amino acids 1-75 (Figure 4f). To further investigate which specific regions of VDAC1 interacted with DsbA-L, we transfected BUMPT cells with the HA-Tag of VDAC1 plasmids with Δ9-13, 22-27, Δ39-45, 55-57, Δ9-13, 22-27, 39-45, 55-57. IP results demonstrated that the anti-HA antibody only precipitated DsbA-L with the Δ39-45 and 55-57 plasmids, and not the Δ9-13 and 22-27 plasmids (see Figure 4g). This further demonstrated that DsbA-L interacted with amino acids 9-13 and 22-27 of VDAC1. Figure 4g features a model showing how DsbA-L interacts with amino acids 9-13 and 22-27 of VDAC1 (Figure 4g). Collectively, these data indicate that DsbA-L interacts with amino acids 9-13 and 22-27 of VDAC1.

Co-localization of DsbA-L or VDAC1 in the mitochondria, and the co-localization of DsbA-L and VDAC1 in (i) BUMPT cells depleted of ATP and (ii) the kidneys of mice and patients

To confirm our IP results, we carried out a co-localization assay. Immunofluorescence confocal microscopy demonstrated that DsbA-L or VDAC1 localized to the mitochondria of BUMPT cells and the kidneys of both sham mice and MCD patients and that this effect was further enhanced in BUMPT cells that had been depleted of ATP, and in the kidneys of mice and patients with AKI (Figure 5 a,b,d,e,g and h). Interestingly, immunofluorescence confocal microscopy verified that the co-localization signal of DsbA-L and VDAC1 in BUMPT cells, and the kidneys of sham mice and MCD patients, was relatively weak. However, the co-localization signal was markedly increased in BUMPT cells that had been depleted of ATP, and in the

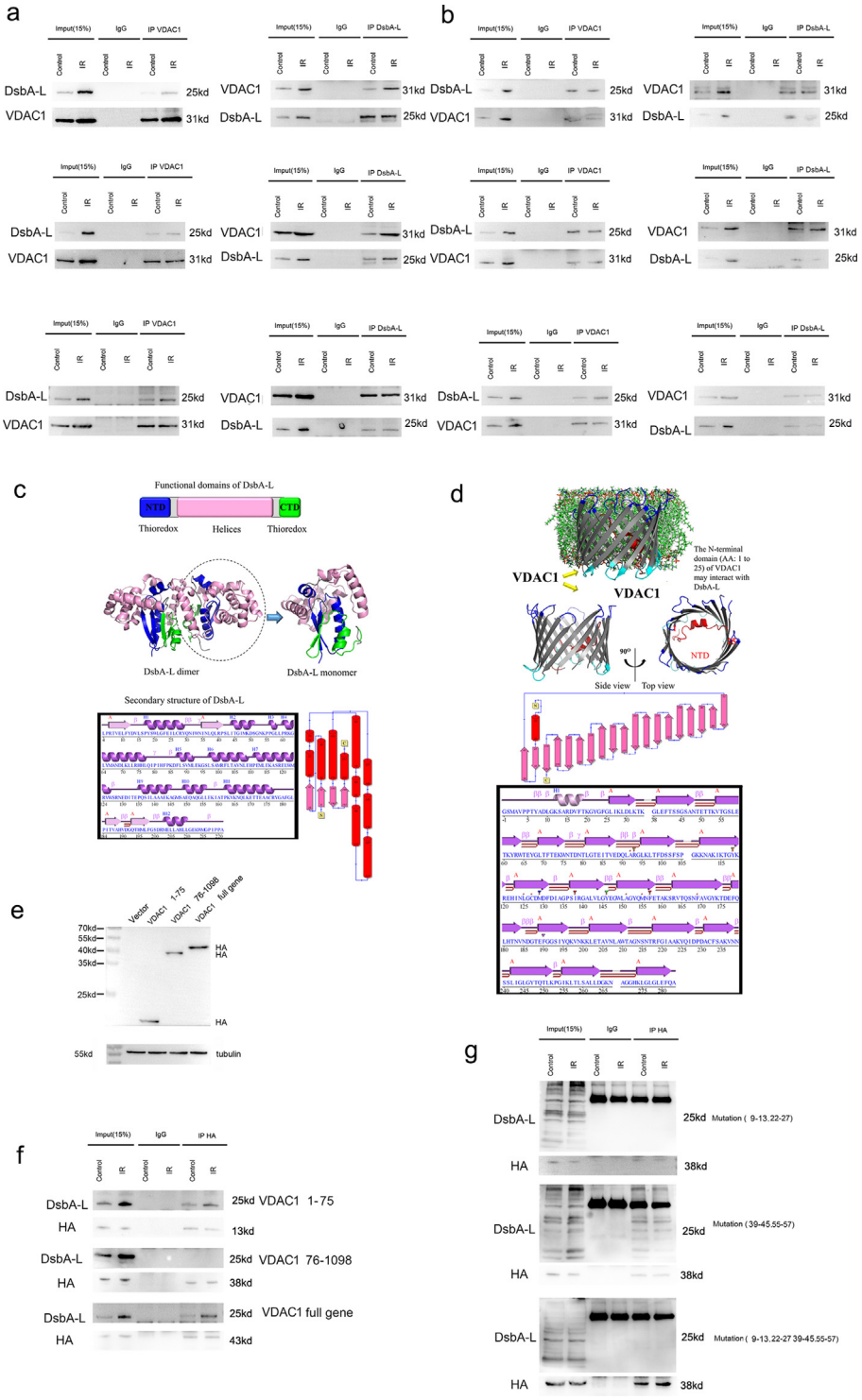

Figure 4. Interaction between DsbA-L and VDAC1 in BUMPT cells with or without ATP depletion and the kidneys of renal I/R mice and patients. (a&b n=3 per group) The whole or mitochondrial lysate was extracted for reciprocal coimmunoprecipitation of DsbA-L and VDAC1 in BUMPT cells treated with ATP depletion and recovery and the kidneys of I/R-induced AKI mice and patients. (c n=3 per group) The functional domains and structure of DsbA-L. (d n=3 per group) The predication model of DsbA-L and VDAC1 interaction. (e−g n=3 per group) Anti-HA immunoprecipitates were analyzed for HA, and then detected for DsbA-L using immunoblotting.

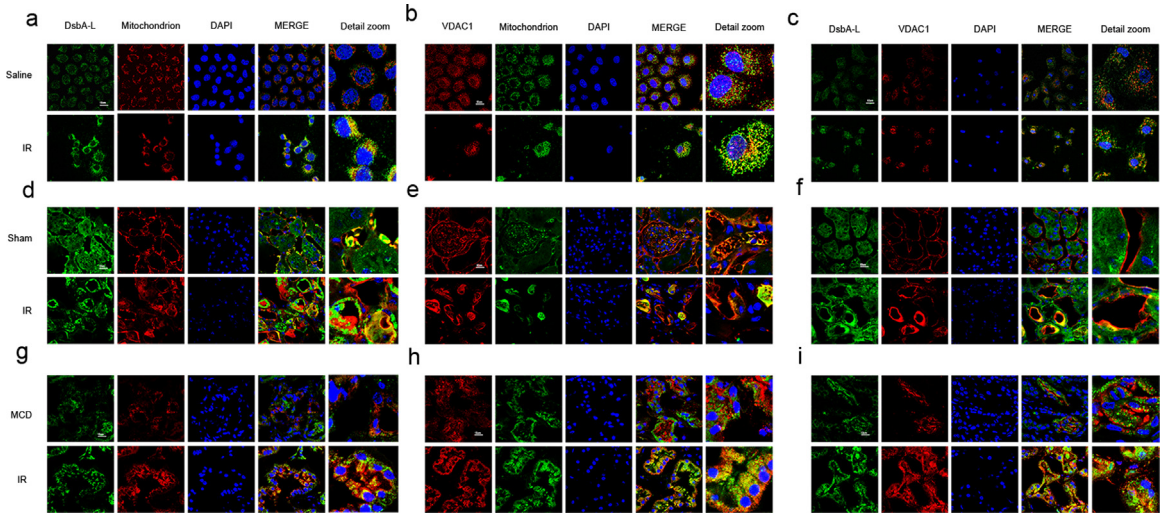

Figure 5. Colocalization of DsbA-L and VDAC1 in the mitochondria of BUMPT cells and kidneys of AKI mice and patients. (a, d&g n=4 per group) Localization of DsbA-L in the mitochondria in BUMPT cells with or without ATP depletion and recovery, the kidneys of mice model in the sham and I/R groups as well as MCD and I/R patients. (b, e&h n=4 per group) Localization of VDAC1 in the mitochondria in BUMPT cells with or without ATP depletion and recovery, the kidneys of mice model in the sham and I/R groups as well as MCD and I/R. (c, f&i n=4 per group) The co-localization of DsbA-L and VDAC1 in the mitochondria in BUMPT cells with or without ATP depletion and recovery, the kidneys of mice model in the sham and I/R groups as well as MCD and I/R patients.

kidneys of mice and patients with AKI (Figure 5 c,f and i). Collectively, these data provide further evidence to support the interaction of DsbA-L and VDAC1 in the mitochondria.

VDAC1-mediated BUMPT cells apoptosis caused by ischemia-reperfusion

Next, we attempted to determine whether VDAC1 was involved in the process of I/R-induced apoptosis in BUMPT cells. Immunoblotting results indicated that VDAC1 expression was induced at I/R 2-0, and reached a peak at I/R 2-2, before then gradually reducing to the levels seen at I/R 2-0 (Figure 6 a and b). FCM analysis showed that I/R induced apoptosis in BUMPT cells; this effect was attenuated by the application of VDAC1 siRNA (Figure 6c). Immunoblotting results further verified that VDAC1 siRNA markedly ameliorated the I/R-induced increase in cleaved caspase-3 expression, the increased accumulation of Bax in the mitochondria, and the increased release of Cyt-c into the cytosol (Figure 6d–k). By contrast, the above changes were enhanced by the overexpression of VDAC1 plasmid (Figure 6 l–s). Together, this data demonstrated that VDAC1-mediated I/R-induced apoptosis in BUMPT cells.

The generation of PT-VDAC1-KO mice

To investigate the role of VDAC1 in AKI, we established a mouse model featuring the knockout of VDAC1 in the proximal tubules of the kidneys. Figure 7a shows the breeding protocol used to generate PT-VDAC1-KO. RT-PCR was used to genotype the PT- VDAC1-KO mice; this was done by amplifying a 416-bp DNA fragment floxed allele and a 370-bp DNA fragment of the Cre gene (Figure 7, b; lanes 4 and 6). The wild-type mice (PT-VDAC1-WT) lacked the Cre gene (Figure 7, b, lanes 2 and 3). Immunoblot analysis indicated that expression levels of VDAC1 in the kidney cortices of the PT-VDAC1-KO mice were lower than those in the PT-VDAC1-WT mice following ischemic or sham treatment (Figure 7 c and d). This was further verified by the immunohistochemical staining of VDAC1 (Figure 7e). These data verified that we had successfully established a PT- VDAC1-KO mouse model.

I/R-induced renal injury, tubular cell apoptosis, and mitochondrial damage, were ameliorated in PT-VDAC1-KO mice

Littermates of the PT-VDAC1-WT and PT- VDAC1-KO mice were treated with ischemia (28 min) followed by reperfusion injury (48 h). We then acquired blood samples and kidney tissues for further examination. We found that PT-VDAC1-KO notably suppressed the I/R-induced elevation in the levels of BUN and creatinine (Figure 8 a and b). Secondly, histological and TUNEL analyses further demonstrated that PT-VDAC1-KO markedly attenuated the I/R-induced tissue damage and renal cell apoptosis (Figure 8 c, d, f and g). Thirdly, EM analyses found that PT-VDAC1-KO significantly attenuated I/R-induced mitochondrial damage (Figure 8 e and h). Finally, immunoblotting confirmed that the

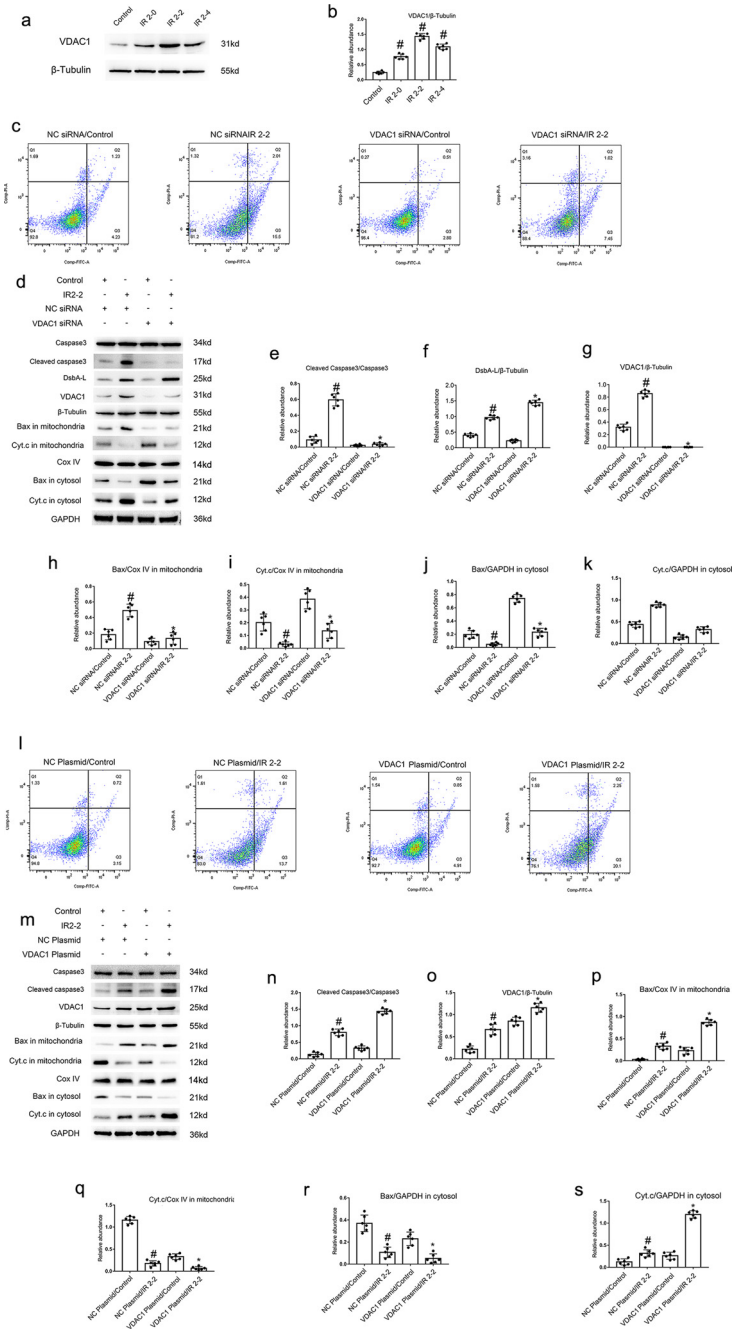

Figure 6. IR-induced expression of cleaved caspase3, BAX, and Cyt-c in BUMPT cells was mediated by VDAC1. The siRNA or plasmid of VDAC1 was transfected into BUMPT cells and then exposed to ATP depletion for 2 h and recovery for 2 h. (a) Immunoblot analysis of VDAC1 and β-tubulin in BUMPT cells. (b) Analysis of the grayscale image between them (c) Flow cytometry analysis of BUMPT cells apoptosis. (d) The immunoblots analysis the expression of cleaved caspase3, VDAC1, and DsbA-L, and the expression of BAX and Cyt-c in mitochondrial and cytosolic fractions. β-tubulin and GAPDH was used as whole lysate or cytosolic loading control, respectively. COX IV was used as mitochondria loading control. (e-k) Analysis of the gray scale image between them. **(i)** Flow cytometry analysis of BUMPT cells apoptosis. (m) The immunoblots analysis the expression of cleaved caspase3, VDAC1, and DsbA-L, and the expression of BAX and Cyt-c in mitochondrial and cytosolic fractions. β-tubulin and GAPDH was used as whole lysate or cytosolic loading control, respectively. COX IV was used as mitochondria loading control. (n-s) Analysis of the gray scale image between them. Each experiment(a,c,d,l & m) was repeated 6 times independently with similar results. Two-tailed Student t-tests was used for two group comparisons. (b), One-way ANOVA was used for the Multiple group comparisons. (e−k and n−s). # $p<0.05$: versus saline group, sham group, or MCD group.# $P<0.05$ versus scramble with saline group. * $P<0.05$ versus scramble with IR group.

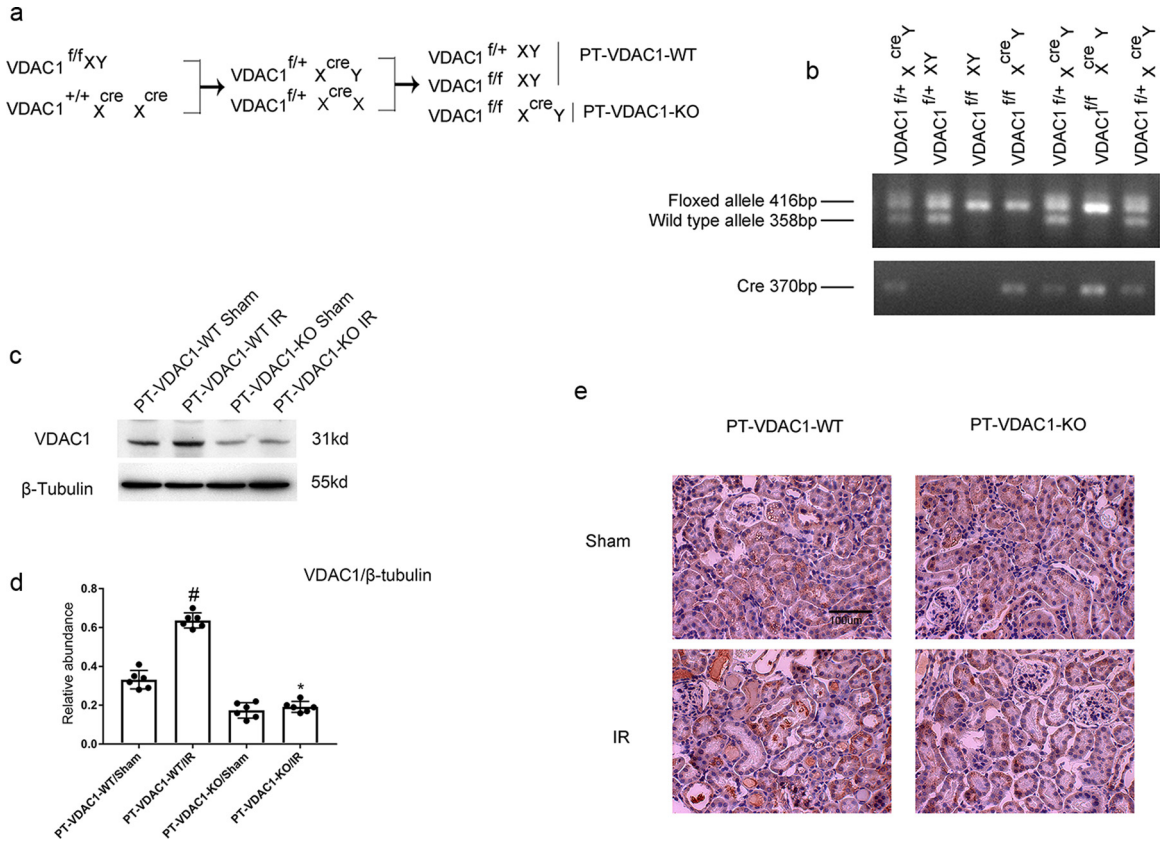

Figure 7. Creation and characteristic of the PT-VDAC1-KO mouse model. (a, b) The breeding protocol for the generation of PT-VDAC1-KO mice and the PCR detection of genotype of wild-type and floxed alleles of VDAC1 and PEPCK-Cre allele. (c) The immunoblot analysis of VDAC1 and β-tubulin using kidney cortical tissues of PT-VDAC1-KO and PT-VDAC1-WT littermate mice following IR injury. (d) Analysis of the grayscale image between them. (e) Immunohistochemical staining of VDAC1 in the kidney cortical tissues of wild-type and VDAC1 mice following IR injury. Original magnification x 400. Scar Bar:100μM. Each experiment(c & e) was repeated 6 times independently with similar results. One-way ANOVA was used for the Multiple group comparisons (d). # $p<0.05$: versus saline group, sham group, or MCD group. # $P<0.05$ versus sham group. * $P<0.05$ versus PT-VDAC1-WT with IR group.

PT-VDAC1-KO mice showed reduced levels of cleaved caspase-3, a lower accumulation of Bax in the mitochondria, and lower rates of Cyt-c release into the cytosol (Figure 8 i–o). These data indicated that VDAC1 also mediated the I/R-induced AKI.

The overexpression of DsbA-L aggravated I/R-induced kidney damage was attenuated in PT-VDAC1-KO mice

Next, we investigated whether VDAC1 mediated the role of DsbA-L during ischemic injury. One week before the mouse model of IR was established, we injected the tail vein of each mouse with the DsbA-L plasmid (the injection was carried out twice during this week). The overexpression of DsbA-L aggravated the IR-induced elevation in BUN and creatinine expression, renal damage, and renal apoptosis; these effects were attenuated in the PT-VDAC1-KO mice (Figure 9 a–d, e and f). Immunoblot results further indicated that the overexpression of DsbA-L enhanced the IR-induced increase in cleaved caspase-3, the accumulation of Bax in the mitochondria, and the release of Cyt-c into the cytosol; these effects were reduced in the PT-VDAC1-KO mice (Figure 9 g and h–l). Collectively, these results further demonstrated that VDAC1 mediated the effect of DsbA-L during ischemic injury.

The attenuation of I/R-induced renal damage in PT-DsbA-L-KO mice was reduced by the overexpression of VDAC1

To further confirm if DsbA-L-mediated tubular damage was dependent on VDAC1, the littermate mice of PT-DsbA-L -WT and PT- DsbA-L -KO mice were first exposed to I/R treatment, and then injected via the tail vein with the VDAC1 overexpression plasmid. The I/R-induced increase in BUN and creatinine levels was ameliorated in the PT- DsbA-L -KO mice; however, this effect was prevented by the overexpression of VDAC1 (Figure 10 a and b). HE and TUNEL staining showed

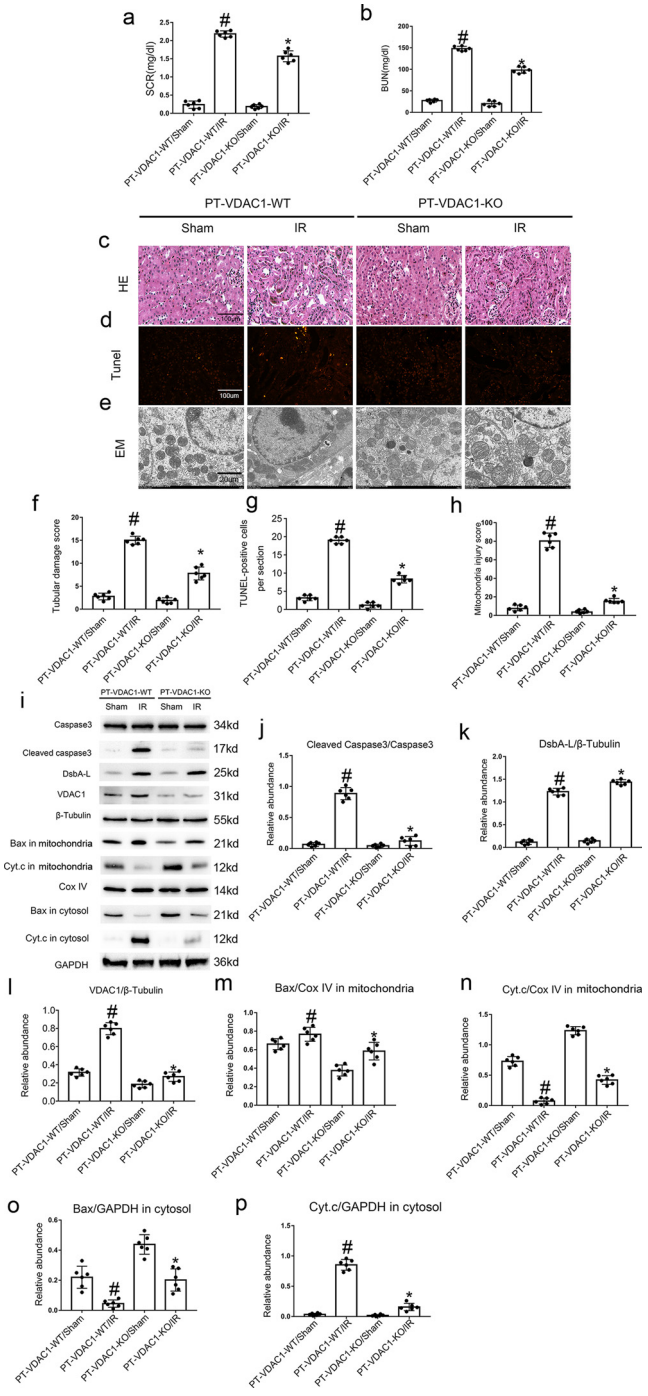

Figure 8. Attenuation of IR-induced renal injury, tubular cell apoptosis, and mitochondrion damage, and the expression of Bax, Cyt-c, and cleaved caspase3 in PT-VDAC1-KO mice. The bilateral renal arteries of PT-VDAC1-KO and PT-VDAC1-WT littermate mice were clamped for 28 min and then released for 48h to establish an IR model. (a) BUN. (b) Serum creatinine. (c) Hematoxylin and eosin staining. (d) Representative sections of TUNEL-positive cells. (e) Electron microscope detection of mitochondrion morphology. (f) Tubular damage score. (g) The number of TUNEL-positive cells. (h) Mitochondria injury score. (i) The immunoblots analysis the expression of cleaved caspase3, VDAC1, and DsbA-L as well as the expression of BAX and Cyt-c in mitochondrial and cytosolic fractions. β-tubulin and GAPDH was used as whole lysate or cytosolic loading control, respectively. COX IV was used as mitochondria loading control. (j−p) Analysis of the grays cale image between them. Original magnification x 400. Scar Bar: 100μM in c & d 20μM in e. Each experiment(c−e&i) was repeated 6 times independently with similar results. One-way ANOVA was used for the Multiple group comparisons (a, b, f−h & j−p). # $p<0.05$: versus saline group, sham group, or MCD group. # $P<0.05$ versus sham group. * $P<0.05$ versus PT-VDAC1 WT with IR group.

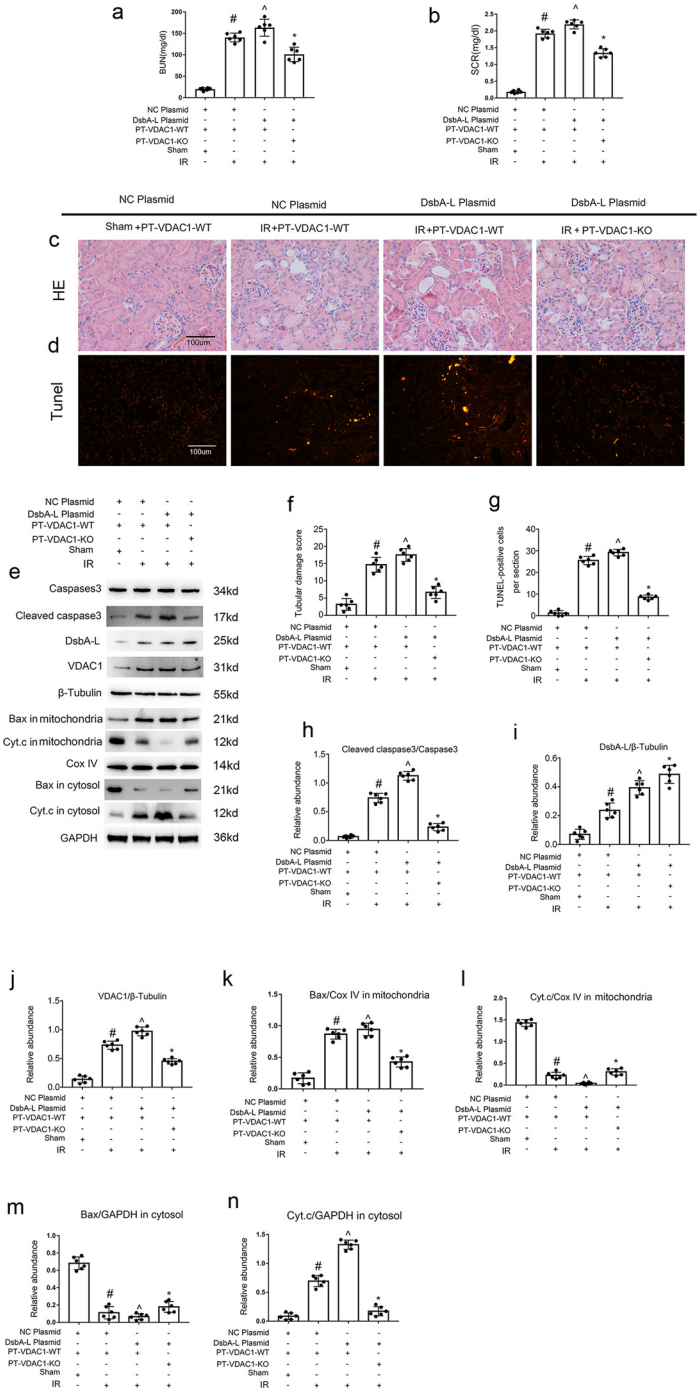

Figure 9. The overexpression of DsbA-L aggravated I/R-induced kidney damage was attenuated in PT-VDAC1-KO mice. The PT-VDAC1-KO and PT-DsbA-L-WT mice were treated with or without DsbA-L plasmid and then established an IR model. (a)BUN. (b) Serum creatinine. (c) Hematoxylin and eosin staining. (d) Representative sections of TUNEL-positive cells. (e) Tubular damage score. (f) The number of TUNEL-positive cells. (g) The immunoblots analysis the expression of cleaved caspase3, VDAC1, and DsbA-L as well as the expression of BAX and Cyt-c in mitochondrial and cytosolic fractions. β-tubulin and GAPDH was used as whole lysate or cytosolic loading control, respectively. COX IV was used as mitochondria loading control. (h−n) Analysis of the gray scale image between them. Original magnification x 400. Scar Bar:100μM. Each experiment(c−e) was repeated 6 times independently with similar results. One-way ANOVA was used for the Multiple group comparisons (a, b and f−n). # $p<0.05$: versus saline group, sham group, or MCD group. # $P<0.05$ versus sham group. ^ $P<0.05$ versus IR group. * $P<0.05$ versus IR group.

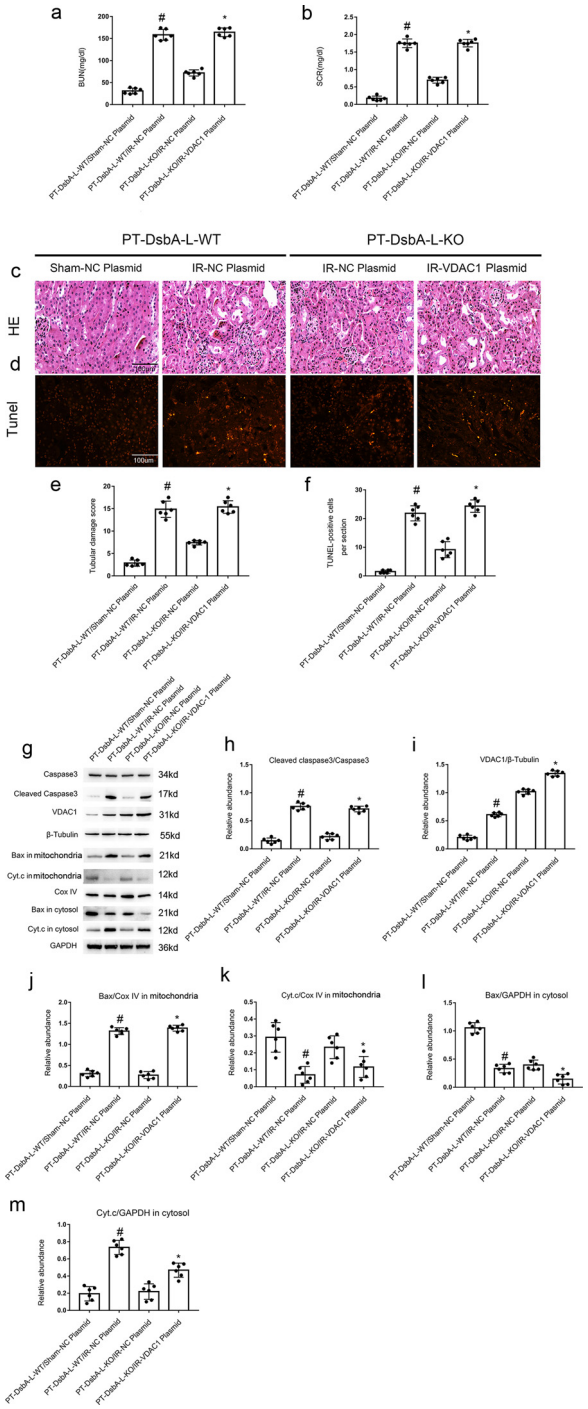

Figure 10. PT-DsbA-L-KO ameliorated IR-induced mice renal injury was diminished by the overexpression of VDAC1. The PT-DsbA-L-KO and PT- DsbA-L-WT mice were treated with or without VDAC1 plasmid and then established an IR model. (a) BUN. (b) Serum creatinine. (c) Hematoxylin and eosin staining. (d) Representative sections of TUNEL-positive cells. (e) Tubular damage score. (f) The number of TUNEL-positive cells. (g) The immunoblots analysis the expression of cleaved caspase3, VDAC1, and DsbA-L as well as the expression of BAX and Cyt-c in mitochondrial and cytosolic fractions. β-tubulin and GAPDH was used as whole lysate or cytosolic loading control, respectively. COX IV was used as mitochondria loading control. (h–m) Analysis of the gray scale image between them. Original magnification x 400. Scar Bar:100μM. Each experiment(c, d and g) was repeated 6 times independently with similar results. One-way ANOVA was used for the Multiple group comparisons (a, b, e, f and h–m). # $p<0.05$: versus saline group, sham group, or MCD group. # $P<0.05$ versus sham group. * $P<0.05$ versus IR group.

that the relative extents of IR-induced renal tissue damage and renal cell apoptosis were reduced in PT- DsbA-L -KO mice and that these effects were blocked by the overexpression of VDAC1 (Figure 10 c–f). Immunoblotting showed that the PT- DsbA-L -KO mice had lower levels of cleaved caspase-3, lower levels of Bax accumulation in the mitochondria, and lower rates of Cyt-c release into the cytosol; however, these effects were eliminated by the overexpression of VDAC1 (Figure 10 g–m). These data supported the fact that DsbA-L promoted ischemic injury in manner that was dependent on VDAC1.

CLP-induced renal injury was attenuated in PT-DsbA-L-KO or PT-VDAC1-KO mice

Sepsis-induced AKI is another common cause of AKI in clinical practice. Littermates of the PT- DsbA-L or VDAC-WT and PT-DsbA-L or VDAC1-KO were subjected to the CLP model and then euthanized 18 h post-surgery. Results indicated that PT-DsbA-L or VDAC1-KO mice markedly reduced the CLP-induced elevations in BUN and creatinine levels, and the increased levels of renal tissue damage and renal cell apoptosis (Figures S1 and S2 a–f). Immunoblotting confirmed that PT-DsbA-L or VDAC1-KO mice also showed reduced levels of cleaved caspase-3, lower levels of Bax accumulation in the mitochondria, and lower rates of Cyt-c release into the cytosol (Figures S1 and S2 g–n). Collectively, these data demonstrated that both DsbA-L and VDAC1 mediated the progression of septic AKI.

VAN-induced renal injury was attenuated in PT-DsbA-L-KO or PT-VDAC1-KO mice

Vancomycin (VAN)-induced AKI is also an important model for AKI. The littermates of PT- DsbA-L or VDAC1-WT and PT-DsbA-L or VDAC1-KO were intraperitoneally injected with VAN (600mg/kg) for 7 consecutive days. The results indicated that PT-DsbA-L or VDAC1-KO mice markedly reduced the VAN-induced elevation of BUN and creatinine levels, renal tissue damage, and renal cell apoptosis (Figures S3 and S4 a–f). Immunoblot analyses further confirmed that PT-DsbA-L or VDAC1-KO mice also showed reduced levels of cleaved caspase-3, a lower extent of Bax accumulation in the mitochondria, and lower rates of Cyt-c release into the cytosol (Figures S3 and S4 g–m). In summary,

these data demonstrated that both DsbA-L and VDAC1 mediated VAN-induced AKI.

DsbA-L mediated I/R induced HK-2 cells apoptosis was associated with VDAC1

The above result found that DsbA-L was involeved in the BUMPT cells apoptosis, however, the function of DsbA in human renal tubular cells remains unclear. DsbA-L siRNA was transfected into HK2 cells, and then exposed ATP depletion for 2 h and recovery for 2 h. The immunoblot results demonstrated that DsbA-L siRNA notably ameliorated I/R-induced increase in cleaved caspase-3 and VDAC1 expression, the increased accumulation of Bax in the mitochondria, and the increased production of Cyt-c into the cytosol (Figure S5 a–h). The data also suggested that the role of DsbA-L in HK2 cells apoptosis was related to the VDAC1 during I/R treatment.

DsbA-L mediated I/R induced HK-2 cells apoptosis is dependent on the VDAC1

To furhter verify whether the role of DsbA-L in HK2 cells apoptosis is depedent on VDAC1. Firsty, HK2 cells were co-transfected with DsbA-L siRNA plus with or without VDAC1 plasmid and then exposed ATP depletion for 2 h and recovery for 2 h. The immunoblot results indicated that DsbA-L siRNA markedly attenuated I/R-induced increase in cleaved caspase-3 and VDAC1 expression, the increased accumulation of Bax in the mitochondria, and the increased production of Cyt-c into the cytosol, this effect was reversed by the overexpression of VDAC1 plasmid (Figure S6a–h). Seacondly, HK2 cells were co-transfected with the VDAC1 siRNA plus with or without DsbA-L plasmid, and then exposed I(2 h)/R(2 h). The immunoblot results showed that VDAC1 siRNA notably ameliorated I/R-induced increase in cleaved caspase-3 and VDAC1 expression, the increased accumulation of Bax in the mitochondria, and the increased production of Cyt-c into the cytosol, this effect was not enhanced by the overexpression of DsbA-L plasmid (Figure S7a–h). The data clearly verified that VDAC1 mediated the pro apoptosis role of DsbA-L in HK-2 cells during I/R treatment.

Discussion

Recent studies found that DsbA-L suppressed the high levels of glucose (HG) induced by renal tubular cell apoptosis and mitochondrial damage in diabetic nephropathy (DN)(18, 37). In the current study, we demonstrated that DsbA-L expression was induced following I/R treatment in BUMPT cells, and the kidneys of both mice and patients (Figure 1). These results confirmed the results of a previous article that reported DsbA-L expression in mitochondria within renal cells (Figure 5).[22] Functionally, we found that DsbA-L-mediated renal cell apoptosis and mitochondrial damage to drive the progression of AKI when induced by ischemia, VAN, and CLP (Figures 2, S1 and S3). However, this action was the opposite of DsbA-L in HG-induced renal cell apoptosis. This difference may be related to the factors sustaining damage and disease type. Mechanistically, we found that DsbA-L interacted with VDAC1 in the mitochondria of renal cells and then induced apoptosis. These findings were further confirmed by ischemia or acute interstitial nephritis (AIN)-induced AKI patients (Figure S8). Collectively, this data demonstrated that DsbA-L could be considered as a new interventional target for AKI.

Previous work reported that DsbA-L played a key protective effect for the kidneys in DN.[37] In contrast, our present study demonstrated that DsbA-L mediated the progression of renal fibrosis in UUO.[22] However, the role of DsbA-L AKI remains largely unknown. In the current study, we found that DsbA-L mediated the progression of AKI. Several lines of evidence supported these findings. First, PT-DsbA-L-KO notably attenuated ischemic AKI (Figure 2). Secondly, the knock down of DsbA-L reduced the I/R-induced apoptosis in BUMPT cells; in contrast, this effect was enhanced by the overexpression of DsbA-L (Figure 3). Thirdly, PT-DsbA-L-KO ameliorated both VAN- and CLP-induced-AKI (Figures S1 and S3). Collectively, this data provided strong evidence to verify that the expression of DsbA-L in the proximal renal tubules plays a pivotal role in AKI.

VDAC1, a multi-functional protein, plays a key role in Ca2+ homeostasis, oxidative stress, and mitochondrial-mediated apoptosis.[19,38–40] A growing body of research has reported that VDAC1 mediates the progression of cancer, neurodegeneration, and myocardial I/R injury.[41–43] However, very little is known about the role of VDAC1 in kidney disease. A recent paper demonstrated that the global deletion of VDAC1 blocked morphological recovery in the proximal tubules, the improvement of kidney function, and enhanced renal fibrosis after ischemic injury.[44] However, the role of VDAC1 in the renal tubules during ischemic injury remains unclear. In the present study, we demonstrated that ischemic injury induced the expression of VDAC1 *in vitro* and enhanced the progression of AKI. Several lines of evidence support the role of VDAC1 in AKI:[1] PT-VDAC1-KO mice showed notable attenuation of I/R-induced AKI (Figure 9)[2]; the inhibition of VDAC1 suppressed I/R-induced apoptosis in BUMPT cells (Figure 6)[3]; CLP and VAN-induced AKI was attenuated by PT- VDAC1-KO (Figures S2 and S3). In addition, global knock out of VDAC1 prevented the repair of mitochondrial damage caused by I/R.[44] Our study demonstrated that the inhibition of VDAC1 markedly attenuated apoptosis in renal cells and the mitochondrial damage induced by ischemic injury, and by CLP- and VAN-injury models, as demonstrated by the lower apoptosis rate, reduced levels of mitochondrial injury, the reduced levels of cleaved caspase-3, the lower extent

of Bax accumulation in the mitochondria, and the lower levels of Cyt-c release into cytosol (Figure S1, S2 and S4). However, the regulation mechanism of VDAC1 for renal cell apoptosis caused by I/R remains unclear in current study, which promoted us to further explore it in future study. Collectively, these data support the fact that the expression of VDAC1 in the renal proximal tubules is involved in the progression of AKI.

The role of DsbA-L in AKI depends predominantly on VDAC1. First, PT-DsbA-L KO mice exhibited marked attenuation of VDAC1 expression in VAN- and CLP-induced AKI (Figures S1 and S3). In contrast, VDAC1 siRNA or PT-VDAC1-KO did not affect the expression of VDAC1 (Figures 6, S2 and S4). Secondly, the overexpression of DsbA-L enhanced the I/R-induced progression of AKI accompanied by an increased level of renal cell apoptosis; this effect was notably reduced in the PT-DsbA-L KO mice (Figure S2). Thirdly, PT-DsbA-L KO attenuated ischemic injury; this was reversed by the overexpression of VDAC1 (Figure 10). Fourthly, DsbA-L siRNA markedly attenuated I/R-induced HK-2 cellls apoptosis, this effect was reversed by the overexpression of VDAC1 plasmid (Figure S6a–h). Fifthly, VDAC1 siRNA notably ameliorated HK-2 cells apoptosis, this was not reinforced by the overexpression of DsbA-L plasmid (Figure S7a–h). These data strongly supported the fact that DsbA-L mediates the progression of AKI by upregulating VDAC1. Whether DsbA-L directly regulates the expression of VDAC1 needs to be investigated further. In the present study, our co-IP results demonstrate that DsbA-L interacted with VDAC1 in the mitochondria of both control and I/R groups from BUMPT cells and the kidneys of mice and patients (Figure 1 a and b). The co-localization of DsbA-L and VDAC1 further confirmed the results arising from co-IP (Figure 5). These experiments could not fully verify a direct interaction between DsbA-L and VDAC1. Bioinformatics prediction, combined with our IP experiments, indicated that DsbA-L interacted with amino acids 9-13 and 22-27 of the VDAC1 protein (Figure 5 c–g). Thus, our data show that DsbA-L interacted directly with VDAC1 to induce renal cell apoptosis and then drive the progression of AKI. In addition, previous study reported that mitochondrial played pivotal role in pathogenesis and recvery during AKI.[45–48] Hence, the data also suggested that DsbA-L interaction with VDAC1 could be considered as a potential therapeutic target to attenuate the pathological mitochondrial effects caused by AKI.

In summary, we demonstrated that proximal tubule-specific DsbA-L KO mice exhibited attenuation of I/R, CLP-, and VAN-induced AKI. Interestingly, we also found that VDAC1 exerts a similar function as DsbA-L. Mechanistically, DsbA-L interacted with VDAC1 and then induced apoptosis in renal cells. Data obtained from both ischemic and AIN tissues demonstrated that the DsbA-L/VDAC1 axis might be involved in human AKI. Our present study demonstrates that this signal pathway may represent a therapeutic target for AKI.

Contributors

DS Zhang conceived and designed the experiments; XZ Li, J Pan, and HL Li carried out the experiments; GD Li, BH Liu, XM Tang, XF Liu, ZB He and ZY Peng analyzed the data; HL Zhang, LX Wang, YJ Li, XD Xiang, XP Chai and YC Yuan contributed reagents and materials, PL Zhen contributed the analysis tools; DS Zhang wrote the main manuscript text but all authors reviewed the manuscript. We declare that all authors read,verified, and approved the final version of the manuscript.

Data sharing statement

The data used and/or analyzed during the current study are available from the corresponding author by reasonable request.

Declaration of interests

The authors have declared that no conflict of interest exists.

Acknowledgements

The study was supported in part by a grant from Key Project of Hunan Provincial Science and Technology Innovation [2020SK1014]. Department of Science and Technology of Hunan Province project of International Cooperation and Exchanges [2020WK2009]. National Natural Science Foundation of China [81870475, 81570646, 81770951]. Changsha Science and Technology Bureau Project [kq2001039]. Natural Science Foundation of Hunan Province [2018JJ2566, 2019JJ40451]. Fundamental Research Funds for the Central Universities of Central South University [2020zzts282, 2021zzts0362]. Supported by Hunan Provincial Innovation Foundation For Postgraduate [CX20200290, CX20210364]. China Hunan Provincial Science and Technology Department [2021SK4004].

Supplementary materials

Supplementary material associated with this article can be found in the online version at doi:10.1016/j.ebiom.2022.103859.

References

1 Zuk A, Bonventre JV. Acute kidney injury. *Annu Rev Med.* 2016;67:293–307.
2 Zhou D, Tan RJ, Lin L, Zhou L, Liu Y. Activation of hepatocyte growth factor receptor, c-met, in renal tubules is required for renoprotection after acute kidney injury. *Kidney Int.* 2013;84(3):509–520.

3 O'Neal JB, Shaw AD, Billings FT. Acute kidney injury following cardiac surgery: current understanding and future directions. *Crit Care*. 2016;20(1):187.
4 Ishimoto Y, Inagi R. Mitochondria: a therapeutic target in acute kidney injury. *Nephrol Dial Transplant*. 2016;31(7):1062–1069. official publication of the European Dialysis and Transplant Association - European Renal Association.
5 Linkermann A, Chen G, Dong G, Kunzendorf U, Krautwald S, Dong Z. Regulated cell death in AKI. *J Am Soc Nephrol*. 2014;25(12):2689–2701.
6 Agarwal A, Dong Z, Harris R, et al. Cellular and molecular mechanisms of AKI. *J Am Soc Nephrol*. 2016;27(5):1288–1299.
7 Morigi M, Perico L, Rota C, et al. Sirtuin 3-dependent mitochondrial dynamic improvements protect against acute kidney injury. *J Clin Investig*. 2015;125(2):715–726.
8 Yu X, Xu M, Meng X, et al. Nuclear receptor PXR targets AKR1B7 to protect mitochondrial metabolism and renal function in AKI. *Sci Transl Med*. 2020;12(543):7591–7605.
9 Stoppe C, Averdunk L, Goetzenich A, et al. The protective role of macrophage migration inhibitory factor in acute kidney injury after cardiac surgery. *Sci Transl Med*. 2018;10(441):4886–4898.
10 Wei Q, Sun H, Song S, et al. MicroRNA-668 represses MTP18 to preserve mitochondrial dynamics in ischemic acute kidney injury. *J Clin Investig*. 2018;128(12):5448–5464.
11 Tran M, Tam D, Bardia A, et al. PGC-1alpha promotes recovery after acute kidney injury during systemic inflammation in mice. *J Clin Investig*. 2011;121(10):4003–4014.
12 Lan R, Geng H, Singha PK, et al. Mitochondrial pathology and glycolytic shift during proximal tubule atrophy after ischemic AKI. *J Am Soc Nephrol*. 2016;27(11):3356–3367.
13 Harris JM, Meyer DJ, Coles B, Ketterer B. A novel glutathione transferase (13-13) isolated from the matrix of rat liver mitochondria having structural similarity to class theta enzymes. *Biochem J*. 1991;278(Pt 1):137–141.
14 Bai J, Cervantes C, Liu J, et al. DsbA-L prevents obesity-induced inflammation and insulin resistance by suppressing the mtDNA release-activated cGAS-cGAMP-STING pathway. *Proc Natl Acad Sci USA*. 2017;114(46):12196–12201.
15 Chen H, Bai J, Dong F, et al. Hepatic DsbA-L protects mice from diet-induced hepatosteatosis and insulin resistance. *FASEB J*. 2017;31(6):2314–2326.
16 Liu M, Xiang R, Wilk SA, et al. Fat-specific DsbA-L overexpression promotes adiponectin multimerization and protects mice from diet-induced obesity and insulin resistance. *Diabetes*. 2012;61(11):2776–2786.
17 Chen X, Han Y, Gao P, et al. Disulfide-bond A oxidoreductase-like protein protects against ectopic fat deposition and lipid-related kidney damage in diabetic nephropathy. *Kidney Int*. 2019;95(4):880–895.
18 Dai XG, Xu W, Li T, et al. Involvement of phosphatase and tensin homolog-induced putative kinase 1-Parkin-mediated mitophagy in septic acute kidney injury. *Chin Med J (Engl)*. 2019;132(19):2340–2347.
19 Shoshan-Barmatz V, Nahon-Crystal E, Shteinfer-Kuzmine A, Gupta R. VDAC1, mitochondrial dysfunction, and Alzheimer's disease. *Pharmacol Res*. 2018;131:87–101.
20 Geisler S, Holmstrom KM, Skujat D, et al. PINK1/Parkin-mediated mitophagy is dependent on VDAC1 and p62/SQSTM1. *Nat Cell Biol*. 2010;12(2):119–131.
21 Lipper CH, Stofleth JT, Bai F, et al. Redox-dependent gating of VDAC by mitoNEET. *Proc Natl Acad Sci USA*. 2019;116(40):19924–19929.
22 Li X, Pan J, Li H, et al. DsbA-L mediated renal tubulointerstitial fibrosis in UUO mice. *Nat Commun*. 2020;11(1):4467.
23 Zhang D, Liu Y, Wei Q, et al. Tubular p53 regulates multiple genes to mediate AKI. *J Am Soc Nephrol*. 2014;25(10):2278–2289.
24 Xu X, Wang J, Yang R, Dong Z, Zhang D. Genetic or pharmacologic inhibition of EGFR ameliorates sepsis-induced AKI. *Oncotarget*. 2017;8(53):91577–91592.
25 Wang J, Li H, Qiu S, Dong Z, Xiang X, Zhang D. MBD2 upregulates miR-301a-5p to induce kidney cell apoptosis during vancomycin-induced AKI. *Cell Death Dis*. 2017;8(10):e3120.
26 Xu L, Li X, Zhang F, Wu L, Dong Z, Zhang D. EGFR drives the progression of AKI to CKD through HIPK2 overexpression. *Theranostics*. 2019;9(9):2712–2726.
27 Zhang P, Yi L, Qu S, et al. The Biomarker TCONS_00016233 drives septic AKI by targeting the miR-22-3p/AIFM1 signaling axis. *Mol Ther Nucleic Acids*. 2020;19:1027–1042.
28 Chen J, Wang J, Li H, Wang S, Xiang X, Zhang D. p53 activates miR-192-5p to mediate vancomycin induced AKI. *Sci Rep*. 2016;6:38868.
29 Xu X, Pan J, Li H, et al. Atg7 mediates renal tubular cell apoptosis in vancomycin nephrotoxicity through activation of PKC-delta. *FASEB J*. 2019;33(3):4513–4524.
30 Lee HT, Emala CW. Preconditioning and adenosine protect human proximal tubule cells in an *in vitro* model of ischemic injury. *J Am Soc Nephrol*. 2002;13(11):2753–2761.
31 Ge Y, Wang J, Wu D, et al. lncRNA NR_038323 Suppresses renal fibrosis in diabetic nephropathy by targeting the miR-324-3p/DUSP1 axis. *Mol Ther Nucleic Acids*. 2019;17:741–753.
32 Wang J, Pan J, Li H, et al. lncRNA ZEB1-AS1 was suppressed by p53 for renal fibrosis in diabetic nephropathy. *Mol Ther Nucleic Acids*. 2018;12:741–750.
33 Song YX, Sun JX, Zhao JH, et al. Non-coding RNAs participate in the regulatory network of CLDN4 via ceRNA mediated miRNA evasion. *Nat Commun*. 2017;8(1):289.
34 Zhu M, Liu J, Xiao J, et al. Lnc-mg is a long non-coding RNA that promotes myogenesis. *Nat Commun*. 2017;8:14718.
35 Kishi S, Brooks CR, Taguchi K, et al. Proximal tubule ATR regulates DNA repair to prevent maladaptive renal injury responses. *J Clin Investig*. 2019;129(11):4797–4816.
36 Briones R, Weichbrodt C, Paltrinieri L, et al. Voltage dependence of conformational dynamics and subconducting states of VDAC-1. *Biophys J*. 2016;111(6):1223–1234.
37 Gao P, Yang M, Chen X, Xiong S, Liu J, Sun L. DsbA-L deficiency exacerbates mitochondrial dysfunction of tubular cells in diabetic kidney disease. *Clin Sci (Lond)*. 2020;134(7):677–694.
38 Shoshan-Barmatz V, Krelin Y, Chen Q. VDAC1 as a player in mitochondria-mediated apoptosis and target for modulating apoptosis. *Curr Med Chem*. 2017;24(40):4435–4446.
39 Ham SJ, Lee D, Yoo H, Jun K, Shin H, Chung J. Decision between mitophagy and apoptosis by Parkin via VDAC1 ubiquitination. *Proc Natl Acad Sci USA*. 2020;117(8):4281–4291.
40 Shoshan-Barmatz V, Krelin Y, Shteinfer-Kuzmine A. VDAC1 functions in Ca(2+) homeostasis and cell life and death in health and disease. *Cell Calcium*. 2018;69:81–100.
41 Magri A, Reina S, De Pinto V. VDAC1 as pharmacological target in cancer and neurodegeneration: focus on its role in apoptosis. *Front Chem*. 2018;6:108.
42 Zhou H, Zhang Y, Hu S, et al. Melatonin protects cardiac microvasculature against ischemia/reperfusion injury via suppression of mitochondrial fission-VDAC1-HK2-mPTP-mitophagy axis. *J Pineal Res*. 2017;63(1).
43 Lin D, Cui B, Ren J, Ma J. Regulation of VDAC1 contributes to the cardioprotective effects of penehyclidine hydrochloride during myocardial ischemia/reperfusion. *Exp Cell Res*. 2018;367(2):257–263.
44 Nowak G, Megyesi J, Craigen WJ. Deletion of VDAC1 hinders recovery of mitochondrial and renal functions after acute kidney injury. *Biomolecules*. 2020;10(4):585–607.
45 Bhargava P, Schnellmann RG. Mitochondrial energetics in the kidney. *Nat Rev Nephrol*. 2017;13(10):629–646.
46 Sun J, Zhang J, Tian J, et al. Mitochondria in Sepsis-Induced AKI. *J Am Soc Nephrol*. 2019;30(7):1151–1161.
47 Tang C, Cai J, Yin XM, Weinberg JM, Venkatachalam MA, Dong Z. Mitochondrial quality control in kidney injury and repair. *Nat Rev Nephrol*. 2021;17(5):299–318.
48 Jiang M, Bai M, Lei J, et al. Mitochondrial dysfunction and the AKI-to-CKD transition. *Am J Physiol Ren Physiol*. 2020;319(6):F1105–F1F16.